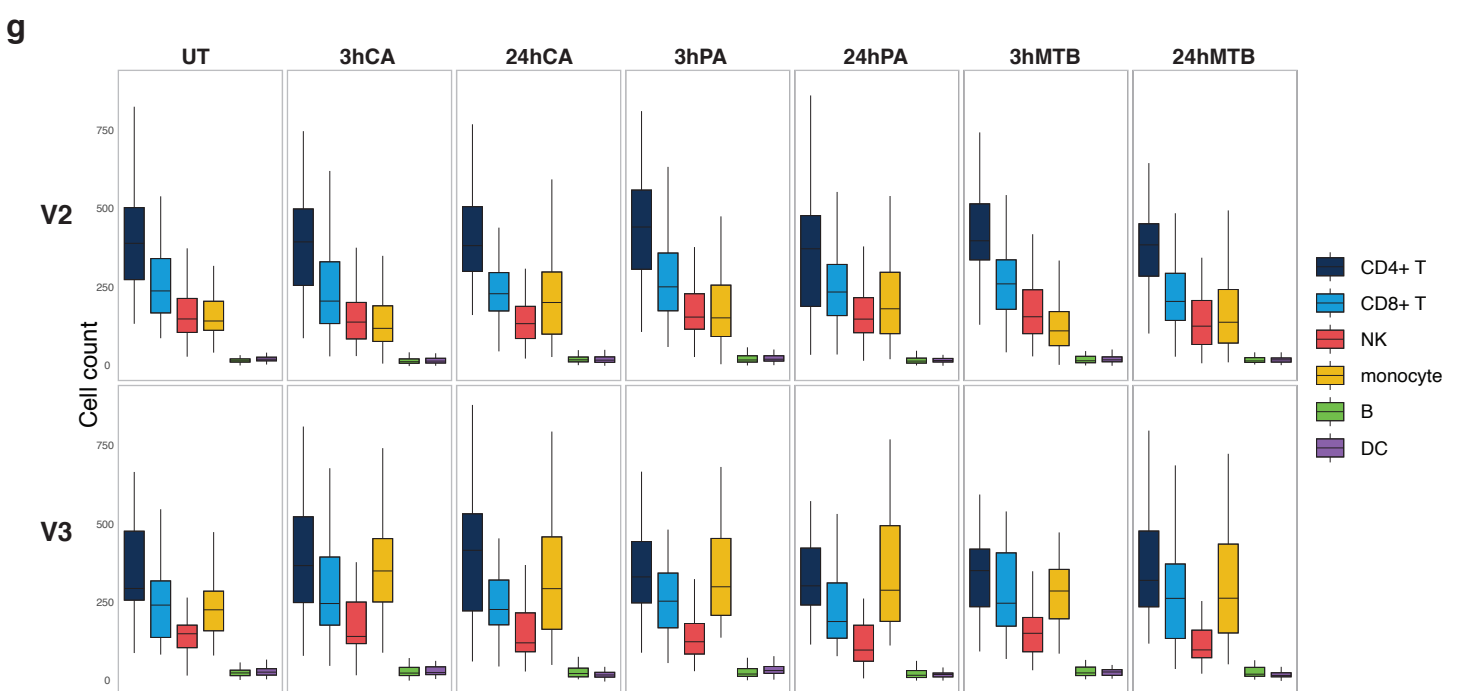
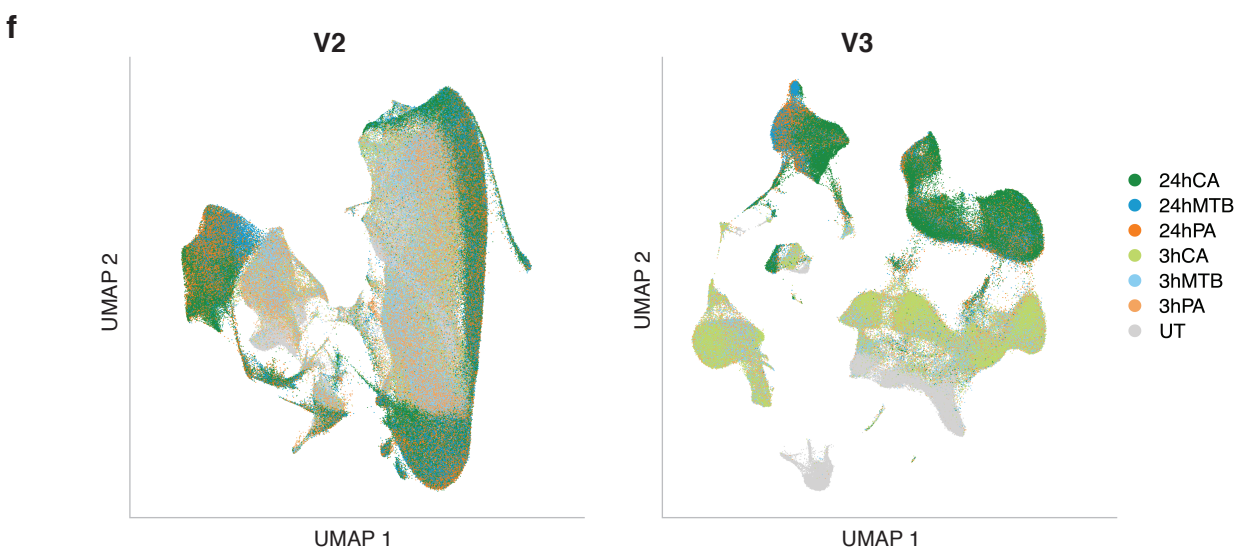
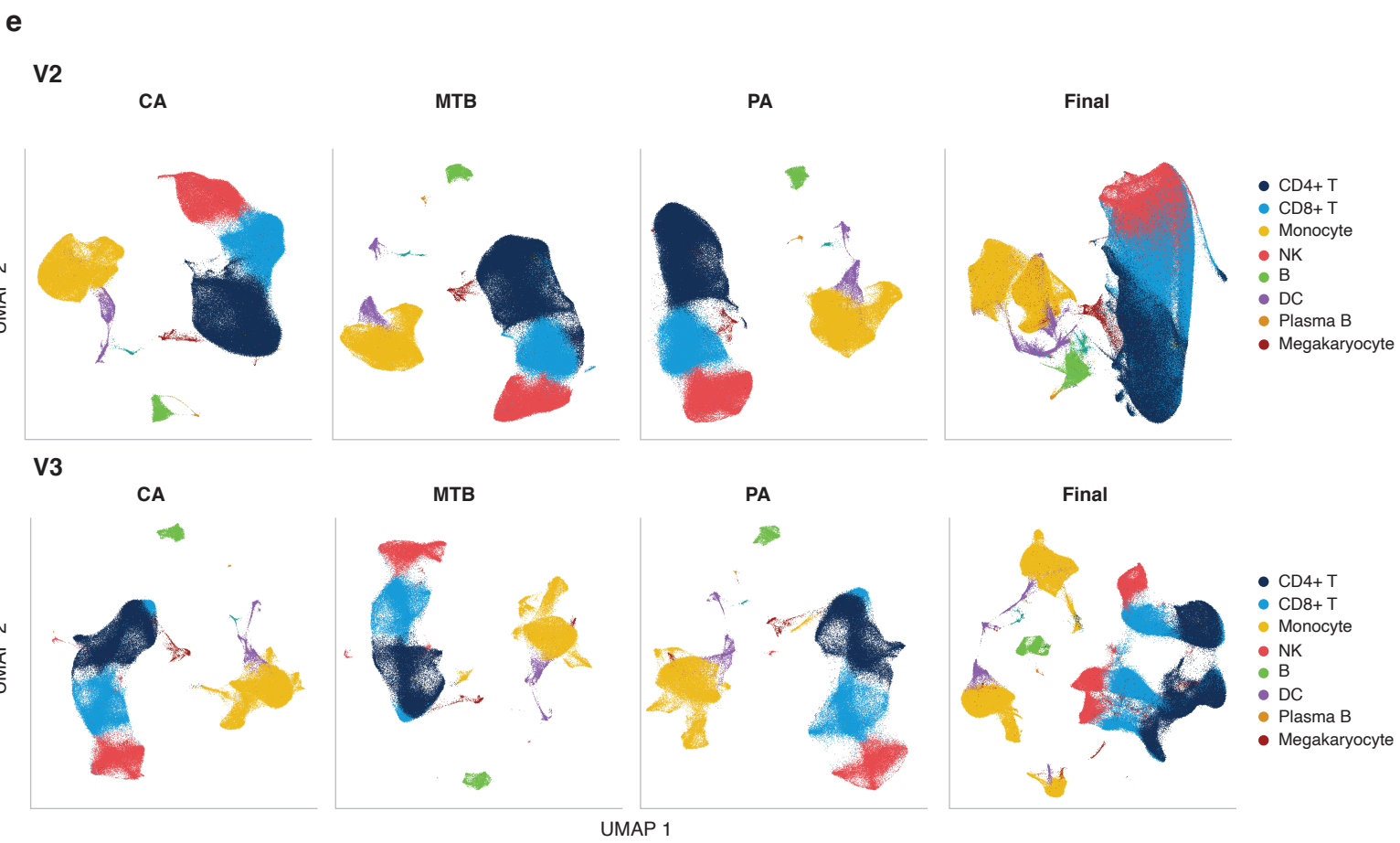
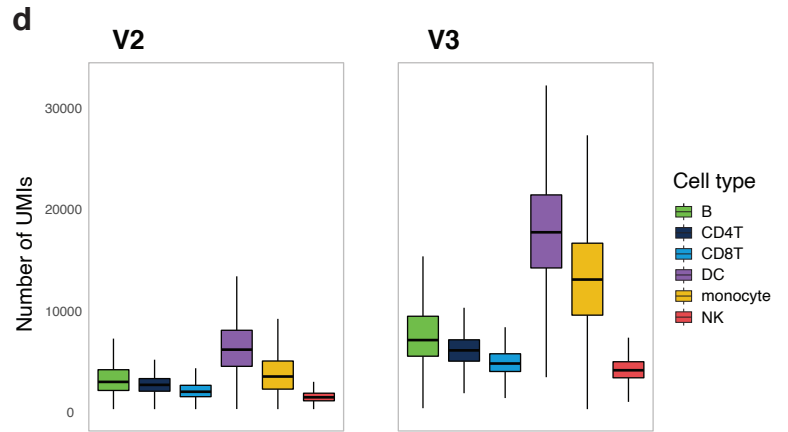
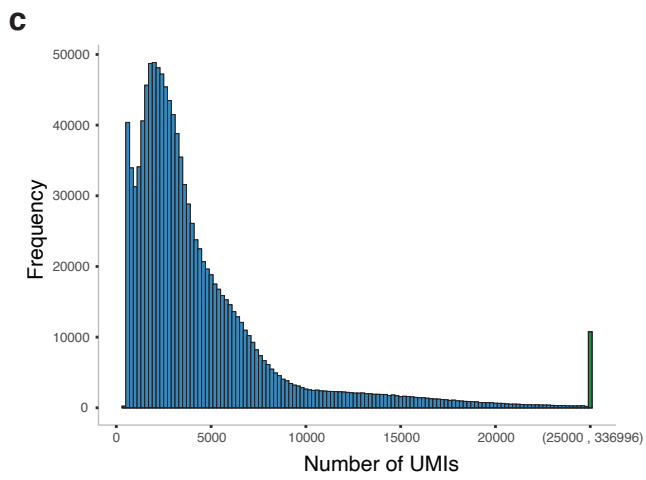
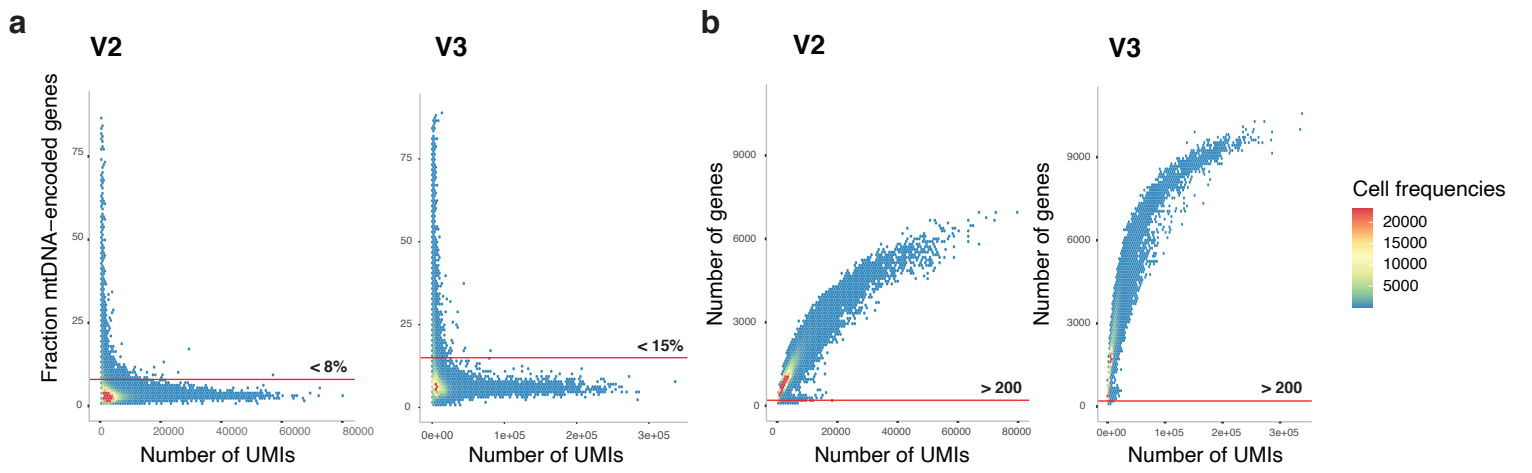


Supplementary Information

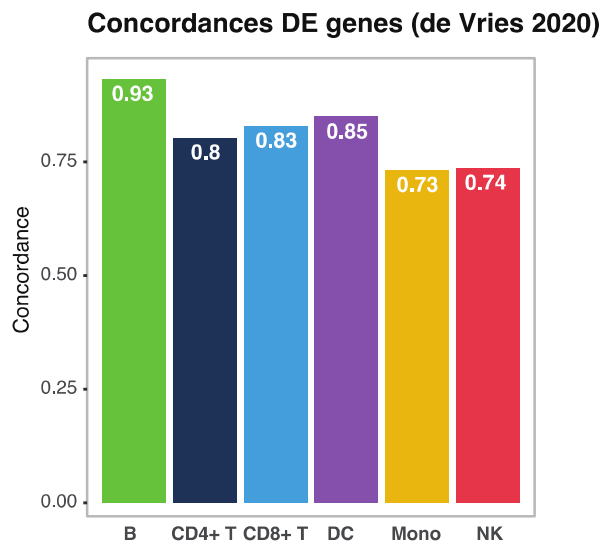
Single-cell RNA-sequencing of peripheral blood mononuclear cells reveals widespread, context-specific gene expression regulation upon pathogenic exposure.

Roy Oelen^{1,2#}, Dylan H. de Vries^{1,2#}, Harm Brugge^{1,2#}, M. Grace Gordon³⁻⁶, Martijn Vochteloo¹, single-cell eQTLGen consortium[§], BIOS Consortium[§], Chun J. Ye^{4,6-10}, Harm-Jan Westra¹, Lude Franke^{1,2*^},
Monique G.P. van der Wijst^{1,2*^}



Supplementary Figure 1. Dataset characteristics

a. The proportion of mitochondrial genes per cell (y-axis) against the number of unique molecular identifiers (UMIs) per cell (x-axis), split per scRNA-seq library chemistry (v2 or v3). Cell density is indicated by color in each graph, going from blue to red for low to high cell numbers, respectively. The red line indicates the QC threshold used for removing cells. **b.** Number of expressed genes versus number of UMIs per cell. Cell density is indicated by color in each graph, going from blue to red for low to high cell numbers, respectively. The red line indicates the QC threshold used for removing cells with a low number of expressed genes. **c.** Distribution of the number of UMIs observed per cell (combining v2 and v3 chemistry). Note that the rightmost bin (green) is larger than the other ones. **d.** Boxplot (showing median, 25th and 75th percentile, and 1.5 x the interquartile range) of the observed number of UMIs per cell, split by cell type and library chemistry. **e.** The UMAP plots per stimulation and library chemistry. Each dot represents a single-cell and the color indicates the assigned cell type. **f.** The integrated UMAP per chemistry where all cells are combined. **g.** Boxplots (showing median, 25th and 75th percentile, and 1.5 x the interquartile range) representing the cell type proportions per individual, split by stimulation-timepoint combination and chemistry. Colors represent the cell types. The number of individuals and cells included in each analysis can be found in the Source Data file.



Supplementary Figure 2. Concordance differential expression results with literature

Bar plot showing the concordance of the identified differentially expressed (DE) genes in this study (as shown in **Supplementary Data 5**) with those identified in de Vries et al. 2020. Each bar represents a different cell type. The number of individuals and cells included in each analysis can be found in the Source Data file.

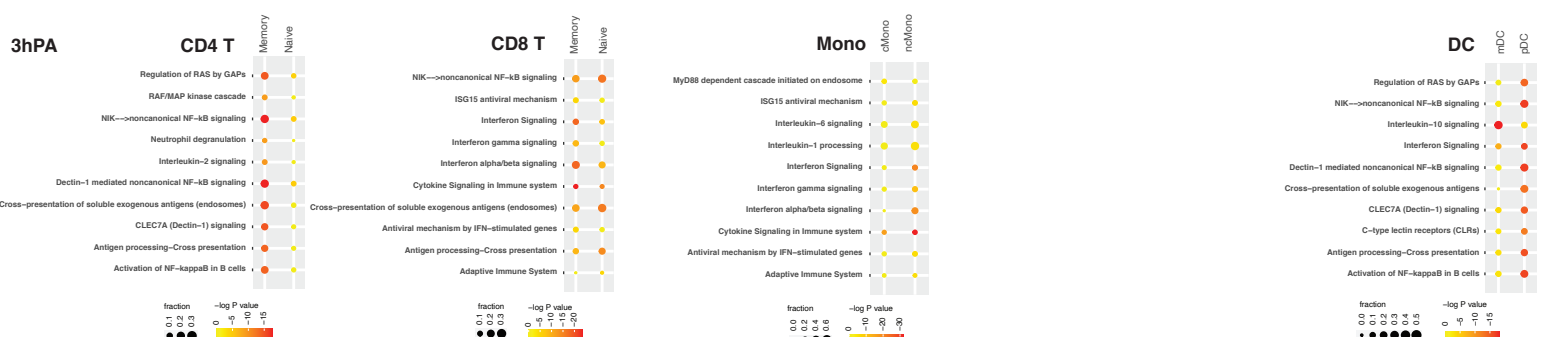
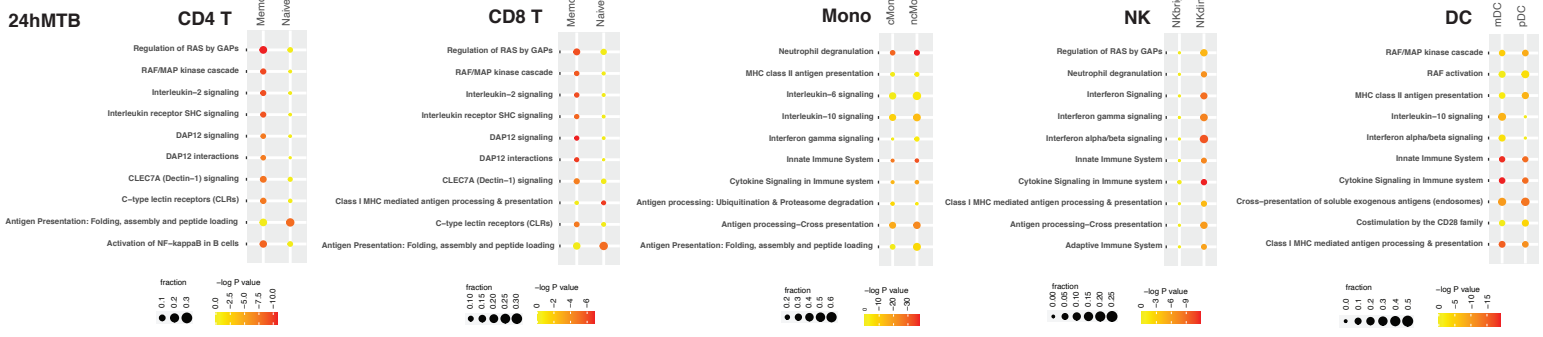
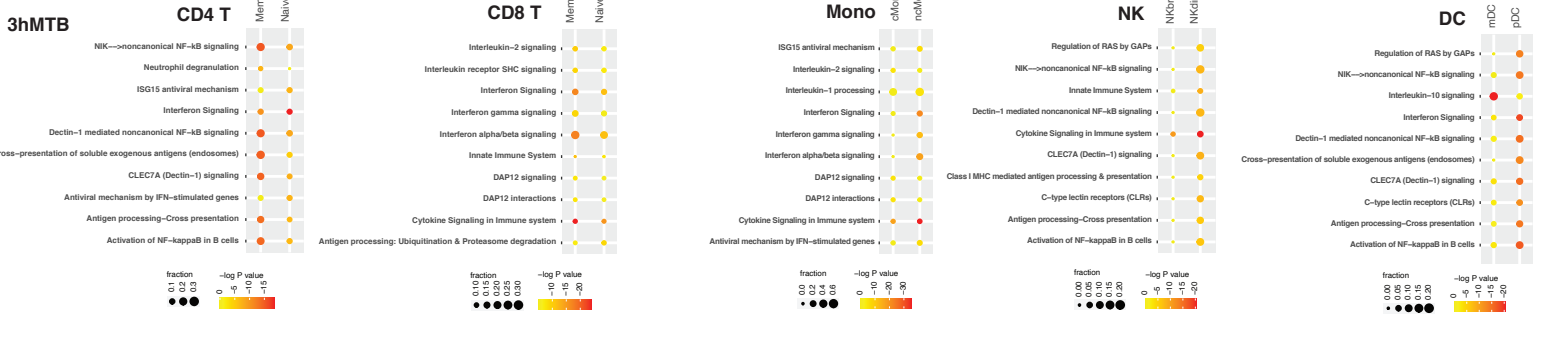
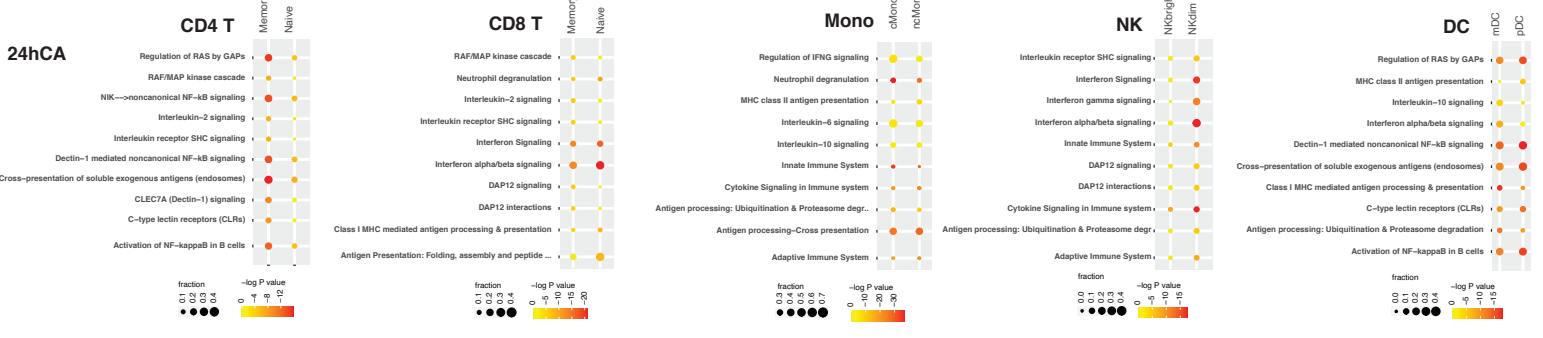
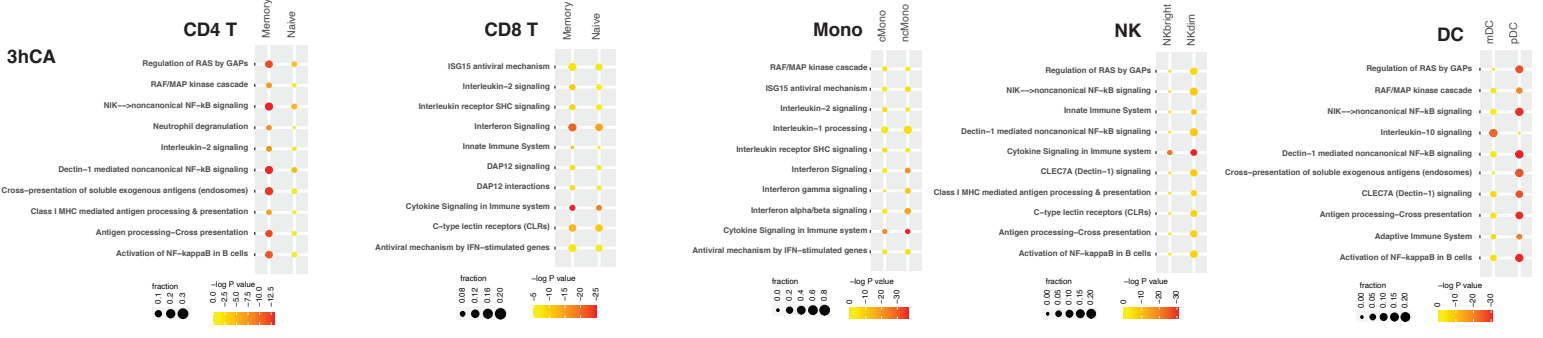
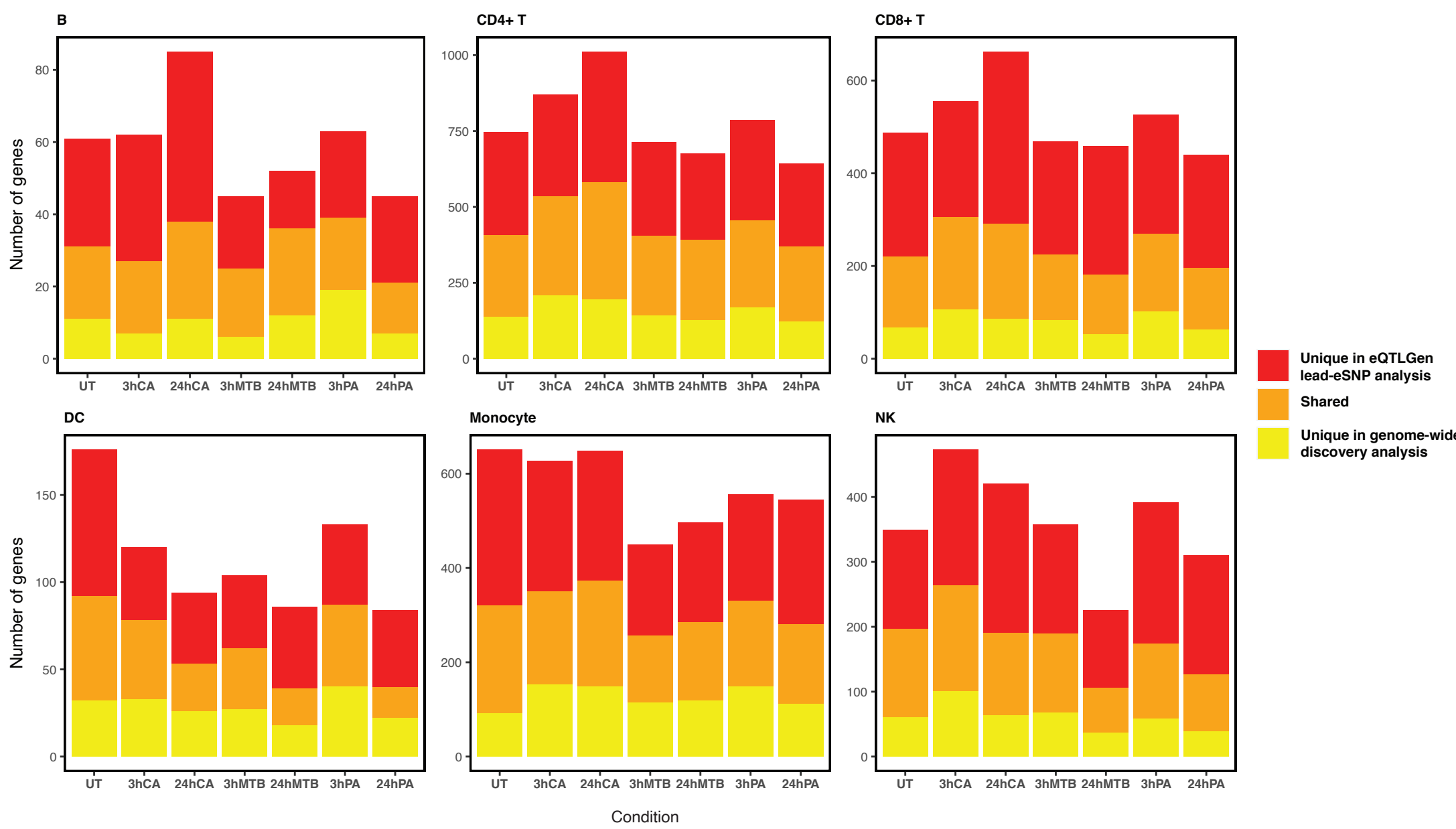


Figure S3. Most differentially enriched pathways in the subcell types

Dotplots of the 10 most enriched pathways with the largest difference in significance between both subcell types, split by subcell type and pathogen stimulation (a complete overview of the enriched pathways can be found in **Table S6**). When subcell type classification provided too few cells or could not be confidently made, no results are shown for that pathogen stimulation. The color indicates the \log_{10} transformed FDR p-value, the size of the dot represents the fraction of DE genes that were found in the total list of genes for the pathway. The number of individuals and cells included in each analysis can be found in the Source Data file.

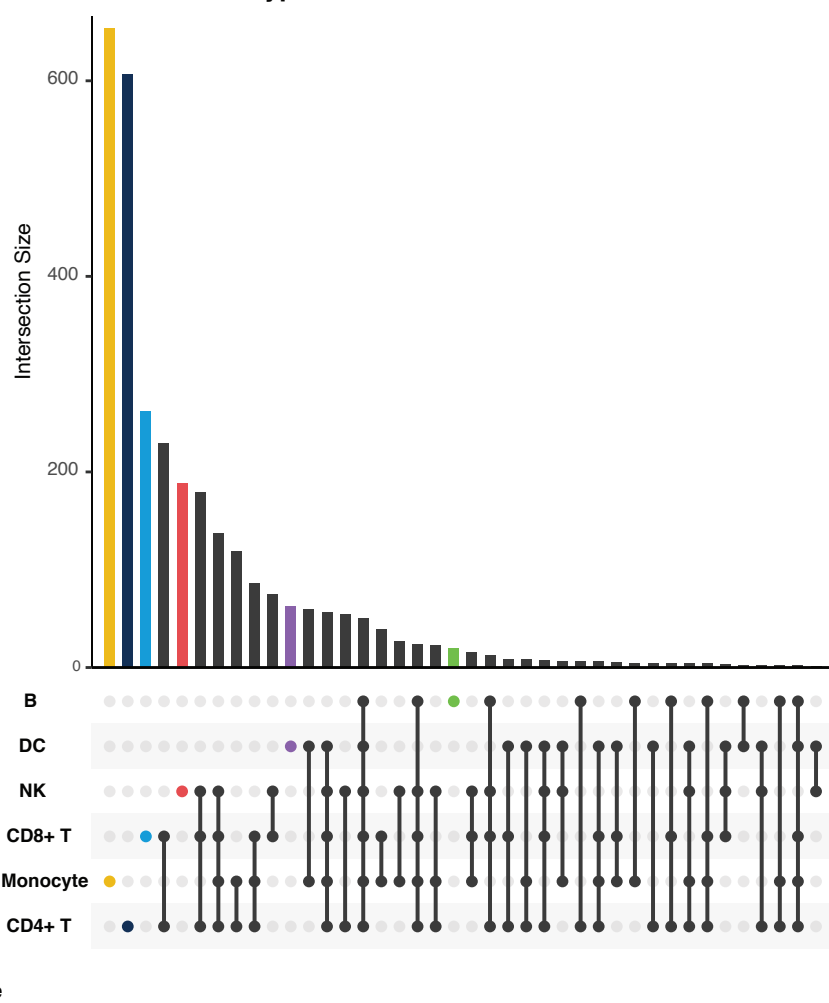
a

Gene sharing of eQTLs between eQTLGen confinement and discovery

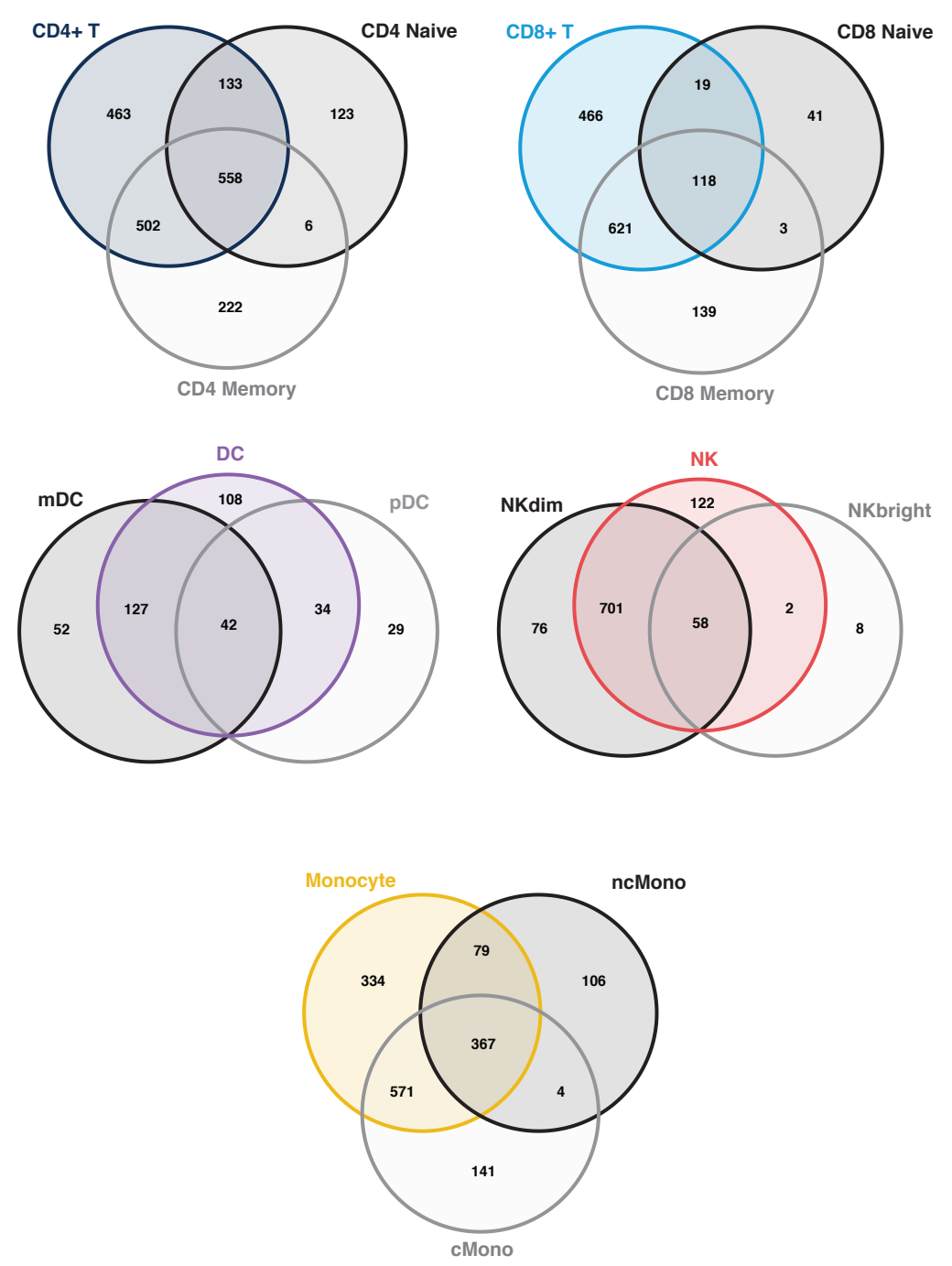


b

Overlap in eQTLs between cell types

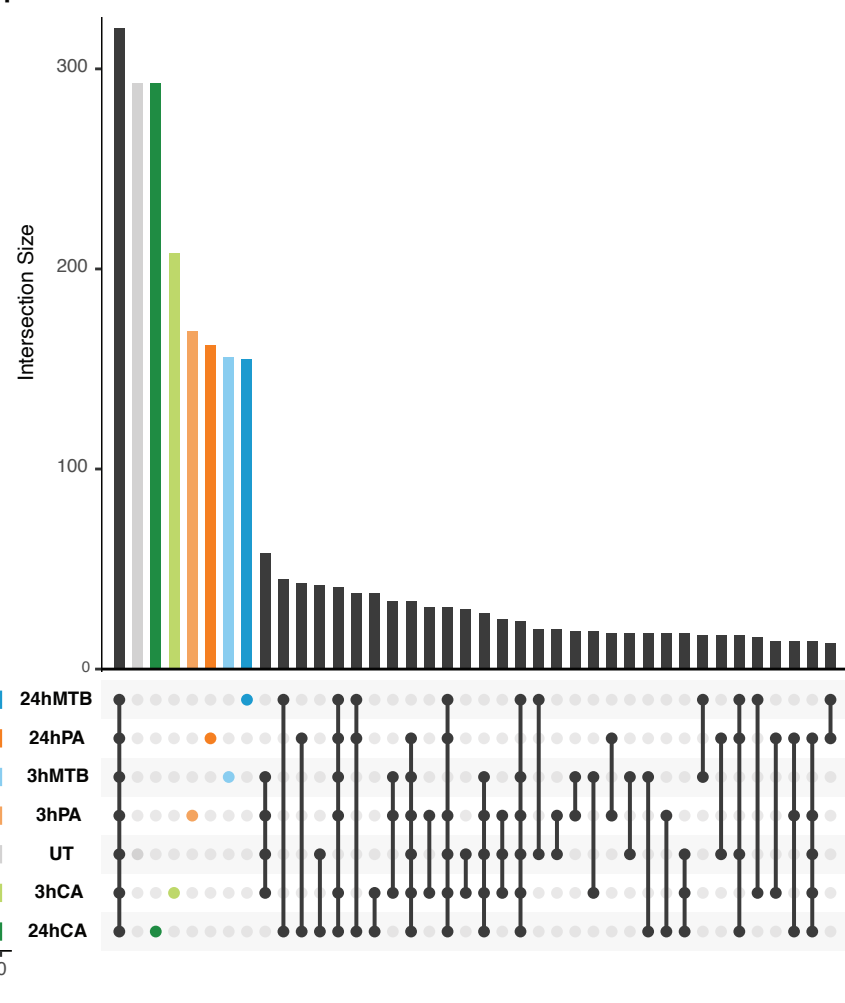


c

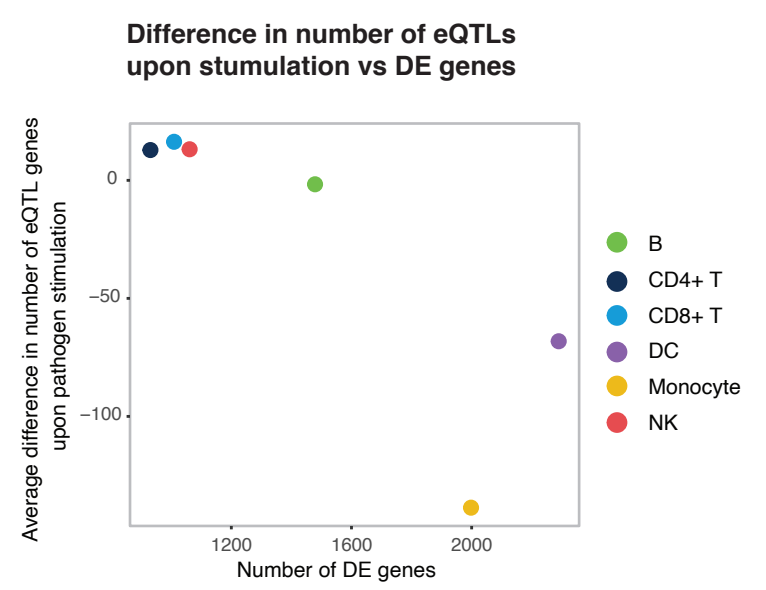


d

Overlap in eQTLs between stimulations

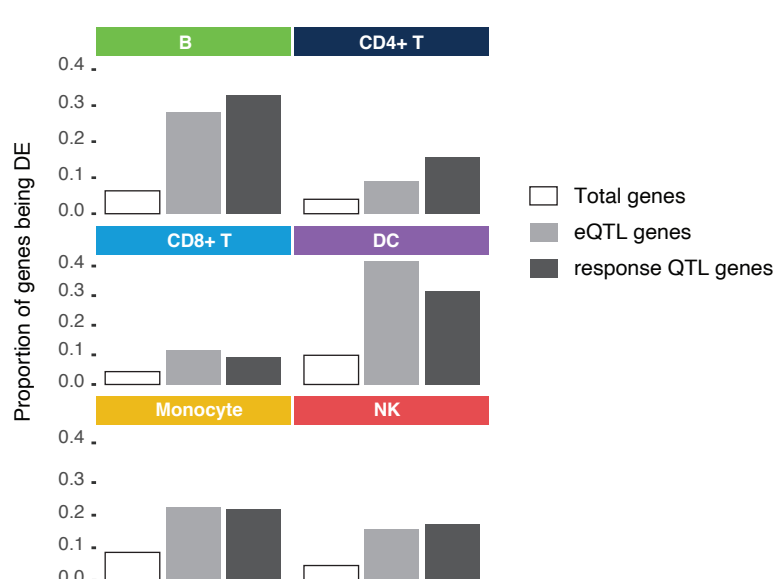


e



f

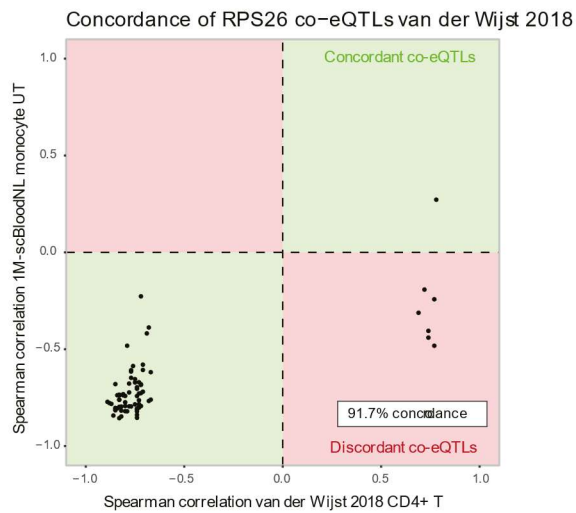
Proportion of genes found as differentially expressed



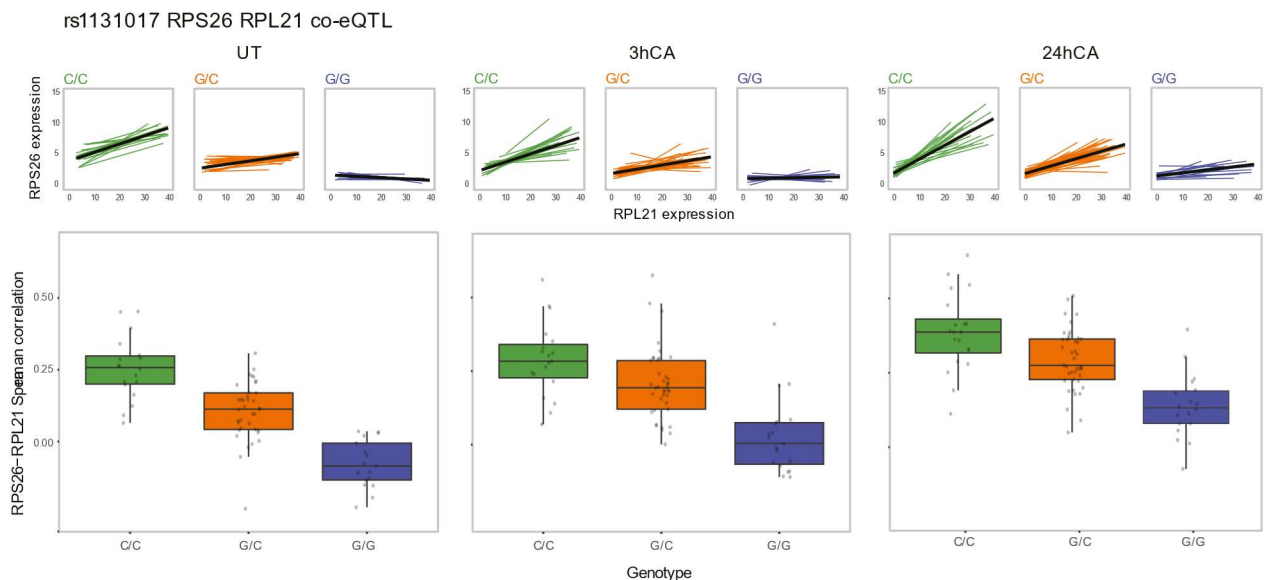
Supplementary Figure 4. eQTL characteristics

a. Stacked bar plots showing the total number of unique eQTL genes per stimulation-timepoint combination within the eQTLGen lead-eSNP confined eQTL analysis (**Supplementary Data 7**) and the genome-wide cis-eQTL discovery analysis (**Supplementary Data 8**). The red color shows eQTL genes that were uniquely identified in the eQTLGen lead-eSNP confined analysis, orange is shared across both analyses and yellow shows eQTL genes that are unique to the genome-wide cis-eQTL discovery analysis. **b.** Overlap of eQTL effects between cell types. Each bar represents the number of eQTLs found for that group, which is indicated by the dots underneath the bar. Colored bars show eQTLs that are unique to one group and black bars are a combination of different groups. **c.** Venn diagrams that show the overlap in identified eQTL genes (in the eQTLGen-confined eQTL analysis) for each major cell type and their two corresponding subcell types. **d.** Overlap of eQTL effects between stimulation-timepoint combinations. Each bar represents the number of eQTLs found for that group, which is indicated by the dots underneath the bar. Colored bars show eQTLs that are unique to one group and black bars are a combination of different groups. **e.** Dot plot showing the difference in number of identified eQTLs upon stimulation (y-axis) compared to the number of DE genes (x-axis). Each dot represents a different cell type, shown by the color. **f.** Bar plots showing the proportion of genes that were identified as DE (**Supplementary Data 5**) per cell type. The three bars represent the complete set of tested genes (white), the complete set of genes with at least one eQTL (gray, **Supplementary Data 7**) and the complete set of genes with at least one response QTL (dark gray, **Supplementary Data 9**). The number of individuals and cells included in each analysis can be found in the Source Data file.

A

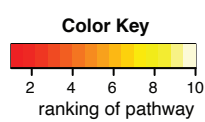


B

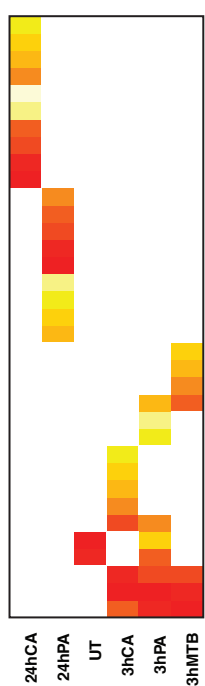


Supplementary Figure 5. RPS26 co-expression QTLs

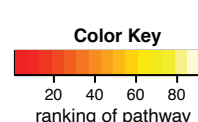
a. Concordance plot comparing Spearman correlations of RPS26 co-expression QTLs in CD4+ T cells from van der Wijst et al. 2018 (x-axis) compared to RPS26 co-expression QTLs in monocytes in the untreated condition of this study. Each dot represents a different co-expression QTL. Dots in green quadrants are concordant and dots in red quadrants are discordant. **b.** The co-expression QTL of RPS26 and RPL21, mediated by rs1131018, across different stimulation-timepoint combinations (meta-analysis p for the UT 1.21×10^{-31} , 3h CA 4.72×10^{-24} , 24h CA 1.28×10^{-5} conditions. Full summary statistics can be found in **Supplementary Data 11**). The top graphs show the individual co-expression, with each colored line representing one individual and the black line showing the regression line across all points. Boxplots (showing median, 25th and 75th percentile, and 1.5 x the interquartile range) representing the Spearman correlations per individual, split by genotype group. Each dot represents the Spearman correlation between RPS26 and RPL21 for one individual within that genotype group. Colors represent the three genotype groups for rs1131018. The number of individuals and cells included in each analysis can be found in the Source Data file.



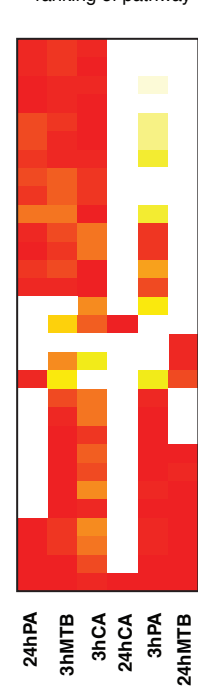
CLEC12A



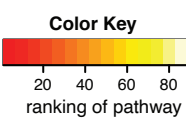
- Metabolism of nucleotides
- TP53 Regulates Metabolic Genes
- Nucleotide-binding domain, leucine rich repeat containing receptor (NLR) signaling pathways
- Detoxification of Reactive Oxygen Species
- Cellular Senescence
- Oxidative Stress Induced Senescence
- Synthesis and interconversion of nucleotide di- and triphosphates
- Inflammasomes
- The NLRP3 inflammasome
- Protein repair
- HIV Life Cycle
- Interleukin-10 signaling
- Chemokine receptors bind chemokines
- Early Phase of HIV Life Cycle
- Binding and entry of HIV virion
- Class A/1 (Rhodopsin-like receptors)
- G alpha (i) signalling events
- HIV Infection
- Peptide ligand-binding receptors
- Abortive elongation of HIV-1 transcript in the absence of Tat
- Antigen Presentation: Folding, assembly and peptide loading of class I MHC
- Regulation of IFNG signaling
- Endosomal/Vacuolar pathway
- Nicotinamide salvaging
- Immunoregulatory interactions between a Lymphoid and a non-Lymphoid cell
- p75NTR signals via NF-kB
- p75NTR recruits signalling complexes
- ER-Phagosome pathway
- Antigen processing-Cross presentation
- Cytokine Signaling in Immune system
- Innate Immune System
- Neutrophil degranulation
- Interferon alpha/beta signaling
- Interferon Signaling
- Interferon gamma signaling



CTSC



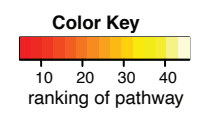
- Selenocysteine synthesis
- Viral mRNA Translation
- Eukaryotic Translation Elongation
- Peptide chain elongation
- Eukaryotic Translation Initiation
- Cap-dependent Translation Initiation
- GTP hydrolysis and joining of the 60S ribosomal subunit
- L13a-mediated translational silencing of Ceruloplasmin expression
- Formation of a pool of free 40S subunits
- Influenza Infection
- Response to elevated platelet cytosolic Ca2+
- Platelet degranulation
- SRP-dependent cotranslational protein targeting to membrane
- Translation
- Metabolism of proteins
- Metabolism of amino acids and derivatives
- Costimulation by the CD28 family
- Endosomal/Vacuolar pathway
- Immunoregulatory interactions between a Lymphoid and a non-Lymphoid cell
- Interleukin-10 signaling
- Signaling by Interleukins
- Interferon alpha/beta signaling
- Interferon gamma signaling
- Interferon Signaling
- Adaptive Immune System
- Cytokine Signaling in Immune system
- Hemostasis
- Platelet activation, signaling and aggregation
- Innate Immune System
- Neutrophil degranulation



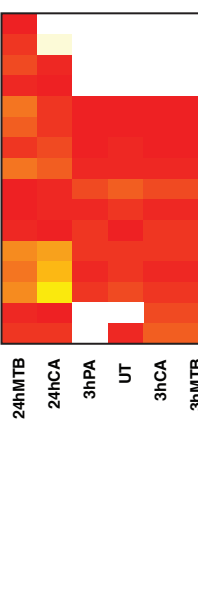
DNAJC15



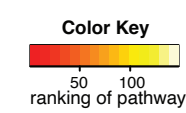
- EPH-Ephrin signaling
- Respiratory electron transport
- The citric acid (TCA) cycle and respiratory electron transport
- Respiratory electron transport, ATP synthesis by chemiosmotic
- Innate Immune System
- EPHB-mediated forward signaling
- TP53 Regulates Metabolic Genes
- Neutrophil degranulation
- Axon guidance
- Infectious disease
- Metabolism of proteins
- SRP-dependent cotranslational protein targeting to membrane
- Disease
- Apoptosis
- Uptake and actions of bacterial toxins
- Uptake and function of diphtheria toxin
- Mitochondrial translation termination
- Mitochondrial translation initiation
- Mitochondrial translation elongation
- Mitochondrial translation
- Organelle biogenesis and maintenance



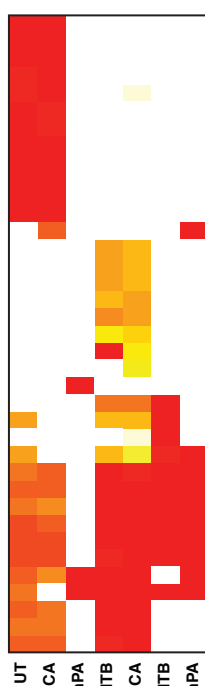
HLA-DQA1



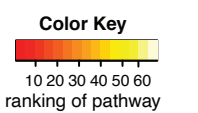
- Endosomal/Vacuolar pathway
- Antigen Presentation: Folding, assembly and peptide loading of class I MHC
- Innate Immune System
- Neutrophil degranulation
- Phosphorylation of CD3 and TCR zeta chains
- Translocation of ZAP-70 to Immunological synapse
- PD-1 signaling
- Generation of second messenger molecules
- Interferon Signaling
- Interferon gamma signaling
- MHC class II antigen presentation
- Downstream TCR signaling
- Costimulation by the CD28 family
- TCR signaling
- Cytokine Signaling in Immune system
- Adaptive Immune System



HLA-DQA2



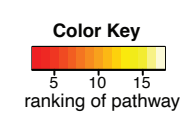
- Response of EIF2AK4 (GCN2) to amino acid deficiency
- Viral mRNA Translation
- Eukaryotic Translation Termination
- SRP-dependent cotranslational protein targeting to membrane
- Nonsense Mediated Decay (NMD) independent of the Exon Junction Complex (EJC)
- Cap-dependent Translation Initiation
- Eukaryotic Translation Initiation
- GTP hydrolysis and joining of the 60S ribosomal subunit
- L13a-mediated translational silencing of Ceruloplasmin expression
- Peptide chain elongation
- Formation of a pool of free 40S subunits
- Eukaryotic Translation Elongation
- Gene and protein expression by JAK-STAT signaling after Interleukin-12 stimulation
- APC/Cdc20 mediated degradation of cell cycle proteins prior to satisfaction of the cell cycle checkpoint
- APC/Cdh1 mediated degradation of Cdc20 and other APC/Cdh1 targeted proteins in late mitosis/early G1
- ABC transporter disorders
- APC/Cdc20 mediated degradation of Securin
- APC/C-mediated degradation of cell cycle proteins
- Interferon alpha/beta signaling
- ABC-family proteins mediated transport
- Immunoregulatory interactions between a Lymphoid and a non-Lymphoid cell
- Interleukin-1 signaling
- Signaling by NOTCH4
- Platelet activation, signaling and aggregation
- MHC class II antigen presentation
- Signaling by Interleukins
- Cytokine Signaling in Immune system
- Interferon Signaling
- Innate Immune System
- Immune System
- Neutrophil degranulation
- Adaptive Immune System
- Interferon gamma signaling
- ER-Phagosome pathway
- Antigen processing-Cross presentation
- Downstream TCR signaling



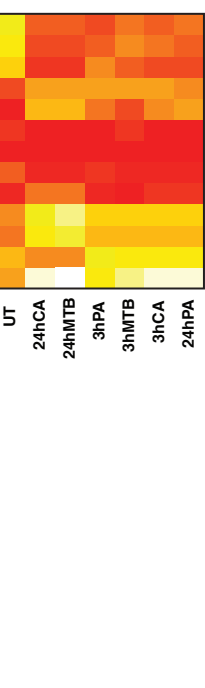
NDUFA12



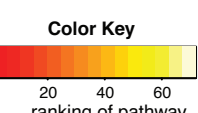
- Influenza Infection
- SRP-dependent cotranslational protein targeting to membrane
- Translation
- Cytokine Signaling in Immune system
- Neutrophil degranulation
- Innate Immune System
- Infectious disease
- Interferon alpha/beta signaling
- Interferon Signaling
- GTP hydrolysis and joining of the 60S ribosomal subunit
- Formation of a pool of free 40S subunits
- Eukaryotic Translation Initiation
- Cap-dependent Translation Initiation
- Influenza Life Cycle
- L13a-mediated translational silencing of Ceruloplasmin expression
- Viral mRNA Translation
- Interferon gamma signaling
- Adaptive Immune System
- Antigen processing-Cross presentation
- Ribosomal scanning and start codon recognition
- Formation of the ternary complex, and subsequently, the 43S complex
- Activation of the mRNA upon binding of the cap-binding complex and eIFs, and subsequent binding to 43S
- Translation initiation complex formation
- Nonsense Mediated Decay (NMD) independent of the Exon Junction Complex (EJC)
- Dissolution of Fibrin Clot
- Interconversion of polyamines



RPS26



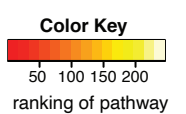
- Nonsense Mediated Decay (NMD) independent of the Exon Junction Complex (EJC)
- Eukaryotic Translation Termination
- Selenocysteine synthesis
- GTP hydrolysis and joining of the 60S ribosomal subunit
- L13a-mediated translational silencing of Ceruloplasmin expression
- Eukaryotic Translation Elongation
- Peptide chain elongation
- Viral mRNA Translation
- Formation of a pool of free 40S subunits
- Eukaryotic Translation Initiation
- Cap-dependent Translation Initiation
- SRP-dependent cotranslational protein targeting to membrane
- Translation



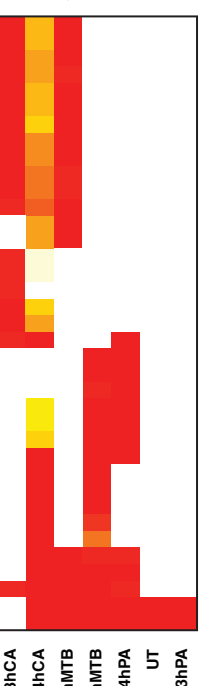
TMEM176A



- Adaptive Immune System
- Transferrin endocytosis and recycling
- Iron uptake and transport
- Antigen processing-Cross presentation
- Membrane Trafficking
- Vesicle-mediated transport
- Respiratory electron transport, ATP synthesis by chemiosmotic coupling, and heat production by uncoupling proteins.
- ROS, RNS production in phagocytes
- Interferon Signaling
- Interferon gamma signaling
- Cytokine Signaling in Immune system
- Response to metal ions
- Metallothioneins bind metals
- Axon guidance
- EPH-Ephrin signaling
- Platelet activation, signaling and aggregation
- Eukaryotic Translation Termination
- Selenocysteine synthesis
- Viral mRNA Translation
- GTP hydrolysis and joining of the 60S ribosomal subunit
- Formation of a pool of free 40S subunits
- Eukaryotic Translation Elongation
- Peptide chain elongation
- Cap-dependent Translation Initiation
- L13a-mediated translational silencing of Ceruloplasmin expression
- SRP-dependent cotranslational protein targeting to membrane
- Nonsense Mediated Decay (NMD) independent of the Exon Junction Complex (EJC)
- Translation
- Infectious disease
- Innate Immune System
- Neutrophil degranulation



TMEM176B



- Eukaryotic Translation Initiation
- Cap-dependent Translation Initiation
- L13a-mediated translational silencing of Ceruloplasmin expression
- Nonsense Mediated Decay (NMD) independent of the Exon Junction Complex (EJC)
- Eukaryotic Translation Termination
- Selenocysteine synthesis
- GTP hydrolysis and joining of the 60S ribosomal subunit
- Viral mRNA Translation
- Peptide chain elongation
- Translation
- Eukaryotic Translation Elongation
- Metabolism of amino acids and derivatives
- Response to elevated platelet cytosolic Ca2+
- Platelet degranulation
- Activation of the mRNA upon binding of the cap-binding complex and eIFs, and subsequent binding to 43S
- Translation initiation complex formation
- Formation of the ternary complex, and subsequently, the 43S complex
- Formation of a pool of free 40S subunits
- SRP-dependent cotranslational protein targeting to membrane
- Metabolism of proteins
- The citric acid (TCA) cycle and respiratory electron transport
- Respiratory electron transport, ATP synthesis by chemiosmotic coupling, and heat production by uncoupling proteins.
- Respiratory electron transport
- EPH-Ephrin signaling
- Membrane Trafficking
- Vesicle-mediated transport
- Adaptive Immune System
- Cytokine Signaling in Immune system
- Interferon Signaling
- Interferon gamma signaling
- TCR signaling
- Downstream TCR signaling
- ER-Phagosome pathway
- Antigen processing-Cross presentation
- Infectious disease
- Innate Immune System
- Neutrophil degranulation

Supplementary Figure 6. Pathway enrichment analysis of co-expression QTL gene sets

Heatmaps showing the enrichment ranks of the pathways associated with the set of co-expressed genes affected by each co-expression QTL gene. Darker colors represent lower ranks, i.e. stronger enrichment, and lighter colors represent higher ranks, i.e. less enrichment. Full summary statistics can be found in **Supplementary Data 6**. The number of individuals and cells included in each analysis can be found in the Source Data file.

Supplementary Note 1. Single-cell eQTLGen Consortium

Cohort collection Yoshinari Ando¹, Odmaa Bayaraa², Irene van Blokland^{3,4}, Mame M. Dieng², Lude Franke^{4,5}, M. Grace Gordon⁶⁻⁹, Hilde E. Groot³, Pim van der Harst¹⁰, Chung-Chau Hon¹, Youssef Idaghdour², Francesca Luca^{11,12}, Vinu Manikanda², Jonathan Moody¹, Martijn C. Nawijn^{13,14}, Yukinori Okada^{15,16}, Woong-Yang Park¹⁷, Roger Pique-Regi^{11,12}, Joseph E. Powell^{18,19}, Deepa Rajagopalan²⁰, Tala Shahin², Jay W. Shin²⁰, Gosia Trynka^{21,22}, Monique G.P. van der Wijst^{4,5}, Seyhan Yazar¹⁸, Jimmie Ye^{7,8,23-26}.

Pipeline development and data analysis José Alquicira-Hernández^{18,27}, Christina B. Azodi^{28,29}, Marijn Berg^{13,14}, Marc Jan Bonder³⁰, Harm Brugge^{4,5}, Anna Cuomo^{18,21}, Ryuya Edahiro^{15,31}, Lude Franke^{4,5}, M. Grace Gordon⁶⁻⁹, Matthias Heinig^{32,33}, Martin Hemberg³⁴, Niek de Klein^{21,22}, Maryna Korshevniuk^{4,5}, Jimmy Tsz Hang Lee²¹, Francesca Luca^{11,12}, Ahmed Mahfouz³⁵⁻³⁷, Davis J. McCarthy^{28,29}, Marta Melé³⁸, Lieke Michielsen³⁵⁻³⁷, Drew Neavin¹⁸, Roy Oelen^{4,5}, Yukinori Okada^{15,16}, Aida Ripoll-Cladellas³⁸, Roger Pique-Regi^{11,12}, Joseph E. Powell^{18,19}, Deepa Rajagopalan²⁰, Oliver Stegle^{21,30,39}, Monique G.P. van der Wijst^{4,5}, Chun J. Ye^{7,8,23-26}.

Steering team Marc Jan Bonder³⁰, Lude Franke^{4,5}, Martin Hemberg³⁴, Ahmed Mahfouz³⁵⁻³⁷, Marta Melé³⁸, Joseph E. Powell^{18,19}, Monique G.P. van der Wijst^{4,5}.

¹ Laboratory for Genome Information Analysis, RIKEN Center for Integrative Medical Sciences, Japan.

² Biology Program, New York University Abu Dhabi, United Arab Emirates.

³ Department of Cardiology, University of Groningen, University Medical Center Groningen, Groningen, the Netherlands.

⁴ Department of Genetics, University of Groningen, University Medical Center Groningen.

⁵ Oncode Institute, Groningen, the Netherlands.

⁶ Biological and Medical Informatics Graduate Program, University of California San Francisco, San Francisco, USA.

⁷ UCSF Division of Rheumatology, Department of Medicine, University of California San Francisco, San Francisco, CA, USA.

⁸ Institute for Human Genetics, University of California San Francisco, USA.

⁹ Department of Bioengineering and Therapeutic Sciences, University of California San Francisco, San Francisco, USA.

¹⁰ Department of Cardiology, University Medical Center Utrecht, Utrecht, the Netherlands.

¹¹ Center for Molecular Medicine and Genetics, Wayne State University School of Medicine, Detroit, USA.

¹² Department of Obstetrics and Gynecology, Wayne State University School of Medicine, Detroit, USA.

¹³ Department of Pathology and Medical Biology, University of Groningen, University Medical Center Groningen, Groningen, the Netherlands.

¹⁴ GRIAC research institute, University Medical Center Groningen, Groningen, the Netherlands.

¹⁵ Department of Statistical Genetics, Osaka University Graduate School of Medicine.

¹⁶ Laboratory for Systems Genetics, RIKEN Center for Integrative Medical Sciences.

¹⁷ Samsung Genome Institute, Samsung Medical Center, Seoul, Korea.

- ¹⁸ Garvan-Weizmann Centre for Cellular Genomics, Garvan Institute of Medical Research, Sydney, Australia.
- ¹⁹ UNSW Cellular Genomics Futures Institute, University of New South Wales, Sydney, Australia.
- ²⁰ A*STAR Genome Institute of Singapore, Singapore.
- ²¹ Wellcome Sanger Institute, Wellcome Genome Campus, Cambridge, UK.
- ²² Open Targets, Wellcome Genome Campus, Cambridge, UK.
- ²³ Bakar Computational Health Sciences Institute, University of California San Francisco, San Francisco, CA, USA.
- ²⁴ Department of Epidemiology and Biostatistics, University of California San Francisco, San Francisco, CA, USA.
- ²⁵ Parker Institute for Cancer Immunotherapy, San Francisco, CA, USA.
- ²⁶ Chan Zuckerberg Biohub, San Francisco, CA, USA
- ²⁷ Computational Genomics, Institute for Molecular Bioscience, University of Queensland, Brisbane, Australia
- ²⁸ St. Vincent's Institute of Medical Research, Fitzroy, Victoria, Australia
- ²⁹ University of Melbourne, Parkville, Victoria, Australia
- ³⁰ Division of Computational Genomics and Systems Genetics, German Cancer Research Center (DKFZ), Heidelberg, Germany.
- ³¹ Department of Respiratory Medicine and Clinical Immunology, Osaka University Graduate School of Medicine.
- ³² Computational Health Center, Helmholtz Zentrum München, Deutsches Forschungszentrum für Gesundheit und Umwelt (GmbH), Munich, Germany.
- ³³ Department of Informatics, Technical University of Munich, Munich, Germany.
- ³⁴ Evergrande Center for Immunologic Disease, Harvard Medical School and Brigham and Women's Hospital, Boston, USA.
- ³⁵ Department of Human Genetics, Leiden University Medical Center, Leiden, The Netherlands.
- ³⁶ Leiden Computational Biology Center, Leiden University Medical Center, Leiden, The Netherlands.
- ³⁷ Delft Bioinformatics Laboratory, Delft University of Technology, Delft, The Netherlands
- ³⁸ Life Sciences Department, Barcelona Supercomputing Center, Barcelona, Catalonia, Spain
- ³⁹ European Molecular Biology Laboratory (EMBL), Genome Biology Unit, Heidelberg, Germany.

Supplementary Note 2. BIOS Consortium (Biobank-based Integrative Omics Study)

Management Team Bastiaan T. Heijmans (chair)¹, Peter A.C. 't Hoen², Joyce van Meurs³, Aaron Isaacs⁴, Rick Jansen⁵, Lude Franke⁶.

Cohort collection Dorret I. Boomsma⁷, René Pool⁷, Jenny van Dongen⁷, Jouke J. Hottenga⁷ (Netherlands Twin Register); Marleen MJ van Greevenbroek⁸, Coen D.A. Stehouwer⁸, Carla J.H. van der Kallen⁸, Casper G. Schalkwijk⁸ (Cohort study on Diabetes and Atherosclerosis Maastricht); Cisca Wijmenga⁶, Lude Franke⁶, Sasha Zhernakova⁶, Etti F. Tigchelaar⁶ (LifeLines Deep); P. Eline Slagboom¹, Marian Beekman¹, Joris Deelen¹, Diana van Heemst⁹ (Leiden Longevity Study); Jan H. Veldink¹⁰, Leonard H. van den Berg¹⁰ (Prospective ALS Study Netherlands); Cornelia M. van Duijn⁴, Bert A. Hofman¹¹, Aaron Isaacs⁴, André G. Uitterlinden³ (Rotterdam Study).

Data Generation Joyce van Meurs (Chair)³, P. Mila Jhamai³, Michael Verbiest³, H. Eka D. Suchiman¹, Marijn Verkerk³, Ruud van der Breggen¹, Jeroen van Rooij³, Nico Lakenberg¹.

Data management and computational infrastructure Hailiang Mei (Chair)¹², Maarten van Iterson¹, Michiel van Galen², Jan Bot¹³, Dasha V. Zhernakova⁶, Rick Jansen⁵, Peter van 't Hof¹², Patrick Deelen⁶, Irene Nooren¹³, Peter A.C. 't Hoen², Bastiaan T. Heijmans¹, Matthijs Moed¹.

Data Analysis Lude Franke (Co-Chair)⁶, Martijn Vermaat², Dasha V. Zhernakova⁶, René Luijk¹, Marc Jan Bonder⁶, Maarten van Iterson¹, Patrick Deelen⁶, Freerk van Dijk¹⁴, Michiel van Galen², Wibowo Arindrarto¹², Szymon M. Kielbasa¹⁵, Morris A. Swertz¹⁴, Erik. W van Zwet¹⁵, Rick Jansen⁵, Peter-Bram 't Hoen (Co-Chair)², Bastiaan T. Heijmans (Co-Chair)¹.

¹ Molecular Epidemiology Section, Department of Medical Statistics and Bioinformatics, Leiden University Medical Center, Leiden, The Netherlands

² Department of Human Genetics, Leiden University Medical Center, Leiden, The Netherlands

³ Department of Internal Medicine, ErasmusMC, Rotterdam, The Netherlands

⁴ Department of Genetic Epidemiology, ErasmusMC, Rotterdam, The Netherlands

⁵ Department of Psychiatry, VU University Medical Center, Neuroscience Campus Amsterdam, Amsterdam, The Netherlands

⁶ Department of Genetics, University of Groningen, University Medical Centre Groningen, Groningen, The Netherlands

⁷ Department of Biological Psychology, VU University Amsterdam, Neuroscience Campus Amsterdam, Amsterdam, The Netherlands

⁸ Department of Internal Medicine and School for Cardiovascular Diseases (CARIM), Maastricht University Medical Center, Maastricht, The Netherlands

⁹ Department of Gerontology and Geriatrics, Leiden University Medical Center, Leiden, The Netherlands

¹⁰ Department of Neurology, Brain Center Rudolf Magnus, University Medical Center Utrecht, Utrecht, The Netherlands

¹¹ Department of Epidemiology, ErasmusMC, Rotterdam, The Netherlands

¹² Sequence Analysis Support Core, Leiden University Medical Center, Leiden, The Netherlands

¹³ SURFsara, Amsterdam, the Netherlands

¹⁴ Genomics Coordination Center, University Medical Center Groningen, University of Groningen, Groningen, the Netherlands

¹⁵ Medical Statistics Section, Department of Medical Statistics and Bioinformatics, Leiden University Medical Center, Leiden, The Netherlands